

Modern Physics Letters B
 © World Scientific Publishing Company

Phase diagram of one-dimensional earth-alkaline cold fermionic atoms

H. Nonne

Laboratoire de Physique Théorique et Modélisation, CNRS UMR 8089, Université de Cergy-Pontoise, Site de Saint-Martin, F-95300 Cergy-Pontoise Cedex, France

E. Boulat

Laboratoire Matériaux et Phénomènes Quantiques, Université Paris Diderot, 2 Place Jussieu, 75205 Paris Cedex 13, France

S. Capponi

Laboratoire de Physique Théorique, Université de Toulouse, UPS (IRSAMC), F-31062 Toulouse, France

P. Lecheminant

Laboratoire de Physique Théorique et Modélisation, CNRS UMR 8089, Université de Cergy-Pontoise, Site de Saint-Martin, F-95300 Cergy-Pontoise Cedex, France

The phase diagram of one-dimensional earth-alkaline fermionic atoms and ytterbium 171 atoms is investigated by means of a low-energy approach and density-matrix renormalization group calculations. For incommensurate filling, four gapless phases with a spin gap are found and consist of two superconducting instabilities and two coexisting bond and charge density-waves instabilities. In the half-filled case, seven Mott-insulating phases arise with the emergence of four non-degenerate phases with exotic hidden orderings.

Keywords: Low-dimensional cold fermionic gases; Exotic Mott-insulating phases.

The recent experimental progresses achieved in trapped ultracold atomic gases augur great opportunities to explore the physics of strong correlations in clean systems and within a wide range of parameters, owing to optical lattices and the high tunability of Feshbach resonances. The attention of the cold atoms community has recently been called to fermionic earth-alkaline atoms such as strontium (Sr) and to atoms endowed with a similar electron structure, such as ytterbium (Yb), which have been cooled down to reach the quantum degeneracy^{1,2}. The interest in those atoms stems from the presence of a ground state 1S_0 (“ g ”) and a metastable excited state 3P_0 (“ e ”) between which transitions are forbidden; moreover, both states have zero electronic angular momentum J , so that the nuclear spin I is decoupled from the electronic spin³. The scattering lengths are independent of the nuclear spins and this results in systems with an extended $SU(N = 2I + 1)$ symmetry that can be realized without any fine-tuning; N can be as large as 10 with ^{87}Sr ($I = 9/2$). In this respect, earth-alkaline cold atoms seem to be very promising

for the experimental realization of high-symmetry systems, and the investigation of exotic many-body physics^{4,5,6,7}.

In this paper, we will focus on the one-dimensional (1D) $N = 2$ case, that is on systems of earth-alkaline like atoms with a nuclear spin $I = 1/2$ such as ^{171}Yb atoms or earth-alkaline atoms where only two nuclear spin states have been trapped. The general N case will be investigated elsewhere. Besides, in addition to the $U(1)_c$ charge symmetry due to the conservation of the total number of atoms, there is also a $U(1)_o$ orbital symmetry, as a result of the conservation of the number of atoms in each state (g and e). These systems display thus an $SU(2)_s \times U(1)_c \times U(1)_o$ continuous symmetry. Moreover, for the sake of simplicity, we assume an extra orbital Z_2 symmetry between the two orbital levels e and g so that they play a similar role. In that case, the effective Hamiltonian model describing such systems loaded in 1D optical lattice is:⁴

$$\begin{aligned} \mathcal{H} = & -t \sum_{i,l\alpha} [c_{l\alpha,i}^\dagger c_{l\alpha,i+1} + \text{H.c.}] - \mu \sum_{i,l} n_{l,i} + \frac{U}{2} \sum_{i,l} n_{l,i} (n_{l,i} - 1) \\ & + V \sum_i n_{g,i} n_{e,i} + V_{\text{ex}} \sum_{i,\alpha,\beta} c_{g\alpha,i}^\dagger c_{e\beta,i}^\dagger c_{g\beta,i} c_{e\alpha,i}, \end{aligned} \quad (1)$$

where $\alpha, \beta = \uparrow, \downarrow$ is the $SU(2)$ spin index and $l = g, e$ represents the two orbital levels. In Eq. (1), $c_{l\alpha,i}^\dagger$ are the four-components fermionic creation operators on site i , and $n_{l,i} = \sum_\alpha c_{l\alpha,i}^\dagger c_{l\alpha,i}$ denotes the density operator on orbital level $l = e, g$ and site i . We intend to investigate the zero-temperature phase diagram of model (1) for incommensurate filling and at half-filling. For this purpose, we will follow a weak-coupling approach, supported by numerical simulations for moderate couplings, using the Density Matrix Renormalization Group (DMRG) algorithm⁸.

1. Incommensurate filling

Since we are interested in the low-energy properties of model (1), the starting point of our approach lies in the weak-coupling regime $|U, V, V_{\text{ex}}| \ll t$. In this regime, only the long-distance properties of the model matter and we perform a continuum limit by linearizing the dispersion relation for non-interacting fermions about the two Fermi points ($\pm k_F$). At incommensurate fillings, there is a spin-charge separation: the charge and the spin, orbital degrees of freedom are decoupled and can be treated separately. The charge degrees of freedom are gapless and exhibit the characteristics of the Luttinger liquid⁹. The low-energy properties of the remaining spin and orbital degrees of freedom can be described in terms of six Majorana (real) fermions $\xi_{R,L}^a$ ($a = 1, \dots, 6$) as in the spin-orbital ladder¹⁰. The interacting part of the

corresponding effective Hamiltonian density reads as follows:

$$\begin{aligned} \mathcal{H}_{so}^{\text{int}} = & \frac{g_1}{2} \left(\sum_{a=1}^3 \xi_R^a \xi_L^a \right)^2 + g_2 \left(\sum_{a=1}^3 \xi_R^a \xi_L^a \right) \left(\sum_{a=4}^5 \xi_R^a \xi_L^a \right) \\ & + \xi_R^6 \xi_L^6 \left[g_3 \sum_{a=1}^3 \xi_R^a \xi_L^a + g_4 \sum_{a=4}^5 \xi_R^a \xi_L^a \right] + \frac{g_5}{2} \left(\sum_{a=4}^5 \xi_R^a \xi_L^a \right)^2, \quad (2) \end{aligned}$$

with $g_1 = -a_0(U + V_{\text{ex}})$, $g_2 = -a_0V$, $g_3 = -a_0(U - V_{\text{ex}})$, $g_4 = -a_0(V - 2V_{\text{ex}})$, and $g_5 = a_0(U - 2V + V_{\text{ex}})$, a_0 being the lattice spacing. The one-loop renormalization group (RG) equations for that model can be found in Ref. 11. The RG analysis leads to the emergence of four different spin-gapped phases. Two phases have coexisting bond and density wave instabilities and can be distinguished by their properties under the Z_2 exchange symmetry ($e \leftrightarrow g$). Spin-Peierls (SP) and charge-density wave (CDW) instabilities are even under Z_2 while SP_π and CDW_π - or orbital-density wave (ODW) - instabilities are odd. Their order parameters are:

$$\begin{aligned} \mathcal{O}_i^{\text{CDW}} &= e^{-2ik_F a_0} \sum_{l,\alpha} c_{l\alpha,i}^\dagger c_{l\alpha,i}, \quad \mathcal{O}_i^{\text{CDW}_\pi} = e^{-2ik_F a_0} \sum_{l,\alpha} \epsilon_l c_{l\alpha,i}^\dagger c_{l\alpha,i}, \\ \mathcal{O}_i^{\text{SP}} &= e^{-2ik_F a_0} \sum_{l,\alpha} c_{l\alpha,i}^\dagger c_{l\alpha,i+1}, \quad \mathcal{O}_i^{\text{SP}_\pi} = e^{-2ik_F a_0} \sum_{l,\alpha} \epsilon_l c_{l\alpha,i}^\dagger c_{l\alpha,i+1}, \quad (3) \end{aligned}$$

with $\epsilon_l = \pm 1$ for $l = g, e$. The SP instability has dimerised pairs of atoms in the g or in the e states; the CDW instability has alternating fully occupied and empty states, and the CDW_π (or ODW) instability is an alternation of sites with two atoms in the g state and sites with two atoms in the e state. Figure 3 (next section) shows a pictorial representation of these instabilities.

The two other phases are superconducting instabilities and differ in the Z_2 exchange symmetry of their pairing operators:

$$\begin{aligned} \mathcal{O}_i^{\text{BCSs}} &= c_{g\uparrow,i+1} c_{e\downarrow,i} - c_{g\downarrow,i+1} c_{e\uparrow,i} - (e \leftrightarrow g), \\ \mathcal{O}_i^{\text{BCSd}} &= c_{g\uparrow,i} c_{e\downarrow,i} - c_{g\downarrow,i} c_{e\uparrow,i}. \quad (4) \end{aligned}$$

The zero-temperature phase diagram is sketched in Fig. 1 depending on the sign of V_{ex} .

2. Half-filling case

2.1. Weak-coupling approach

At half-filling, there is no spin-charge separation anymore since umklapp processes couple these degrees of freedom in sharp contrast to the half-filled Hubbard chain⁹. The interplay between charge and spin-orbital degrees of freedom can be investigated by introducing two additional Majorana fermions $\xi_{R,L}^{7,8}$ for the charge sector. The umklapp processes generate new terms which add to the effective

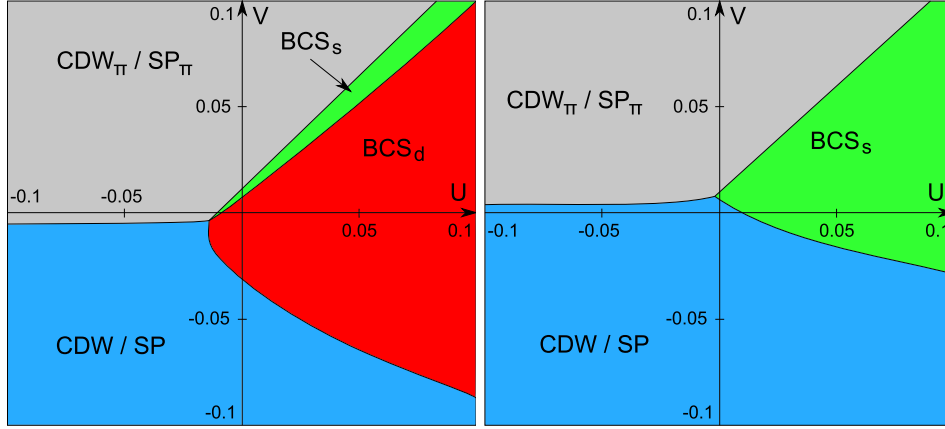


Fig. 1. Phase diagram of model (1) at incommensurate filling for $V_{\text{ex}} = -0.01t$ (left) and $V_{\text{ex}} = 0.01t$ (right).

interacting Hamiltonian (2):

$$\mathcal{H}_{\text{umklapp}} = \frac{g_6}{2} \left(\sum_{a=7}^8 \xi_R^a \xi_L^a \right)^2 + (\xi_R^7 \xi_L^7 + \xi_R^8 \xi_L^8) \left[g_7 \sum_{a=1}^3 \xi_R^a \xi_L^a + g_8 \sum_{a=4}^5 \xi_R^a \xi_L^a + g_9 \xi_R^6 \xi_L^6 \right], \quad (5)$$

where $g_6 = a_0(U + 2V - V_{\text{ex}})$, $g_7 = a_0(V - V_{\text{ex}})$, $g_8 = a_0U$, and $g_9 = a_0(V + V_{\text{ex}})$. The analysis of the one-loop RG equations for the Majorana models (2, 5) is detailed in Ref. ¹². The resulting zero-temperature phase diagram is depicted in Fig. 2,

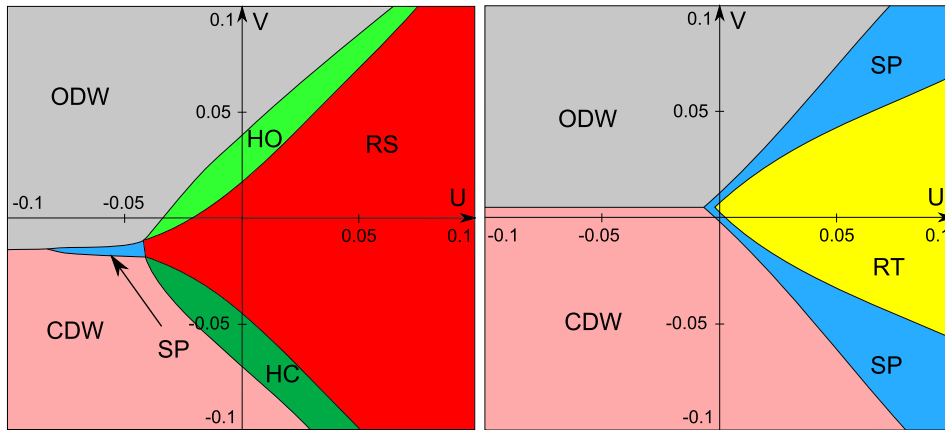


Fig. 2. Phase diagram of model (1) at half-filling for $V_{\text{ex}} = -0.03t$ (left) and $V_{\text{ex}} = 0.01t$ (right).

Seven Mott-insulating phases have been found in the phase diagram, all fully gapped in charge, orbital, and spin degrees of freedom; three of them are two-fold degenerate and four are non-degenerate. As regards the three degenerate phases, depicted in Fig. 3, their order parameters were given in Eq. (3): one is the SP phase ($\mathcal{O}_i^{\text{SP}}$), a second one is the CDW phase ($\mathcal{O}_i^{\text{CDW}}$), and the third one is the ODW phase ($\mathcal{O}_i^{\text{ODW}} = \mathcal{O}_i^{\text{CDW}\pi}$). In the incommensurate case, these orders have a power-law decay while true long-range ordering occurs in the half-filled case.

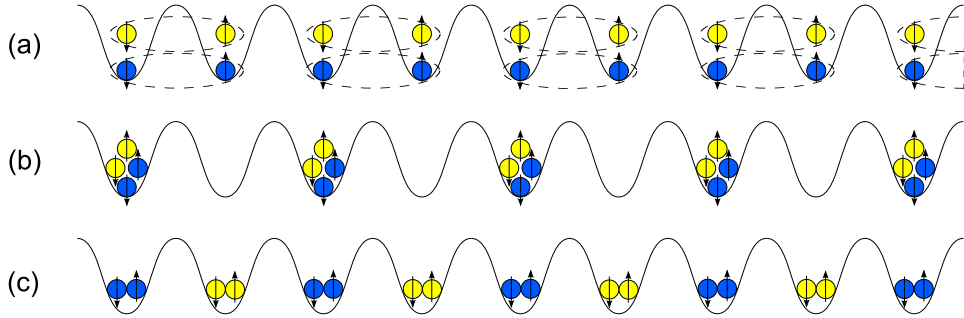


Fig. 3. (color online) The blue atoms are in the ground state, and the yellow color represents the excited state. (a) The SP phase contains dimerised pairs of atoms in the g or in the e states; (b) the CDW phase swings between fully occupied and empty states; (c) the ODW is an alternation of sites with two atoms in the g state and sites with two atoms in the e state.

The first non-degenerate phase is the rung triplet (RT) phase, so called since it is related to the RT phase of the two-leg spin-1/2 ladder, with the orbital states g, e playing the role of the legs. This gapped phase is adiabatically connected to the Haldane phase of the spin-1 Heisenberg chain⁹ and displays a dilute order which consists in an alternation of $S^z = S_g^z + S_e^z = +1$ (with $S_i^z = [c_{l\uparrow,i}^\dagger c_{l\uparrow,i} - c_{l\downarrow,i}^\dagger c_{l\downarrow,i}]/2$) and $S^z = -1$ states with an arbitrary number of $S^z = 0$ states in between (see Fig. 4 (a)). The second non-degenerate phase is a rung singlet (RS) phase where the two orbital states form a spin singlet state on each site (Fig. 4 (b)). The third phase is called Haldane charge (HC) phase since it belongs to the same type as the Haldane (spin) phase above, but now, the correct quantum number to characterize the dilute order is the occupation number n_i . States with $n_i = 4$ and $n_i = 0$ alternate, and there is an arbitrary number of singlet ($n_i = 2$) states in between. It is easily seen (Fig. 4 (c)) that HC interpolates between the CDW and the RS phase. This HC phase has been first identified in the context of 1D spin-3/2 cold alkaline fermions¹³. Finally, the last non-degenerate phase is called Haldane orbital (HO) and the alternation takes place between states with $(n_g - n_e)/2 = \pm 1$ with again an arbitrary number of spin singlets $(n_g - n_e)/2 = 0$ in between (Fig. 4 (d)). This phase interpolates between the ODW and the RS phases.

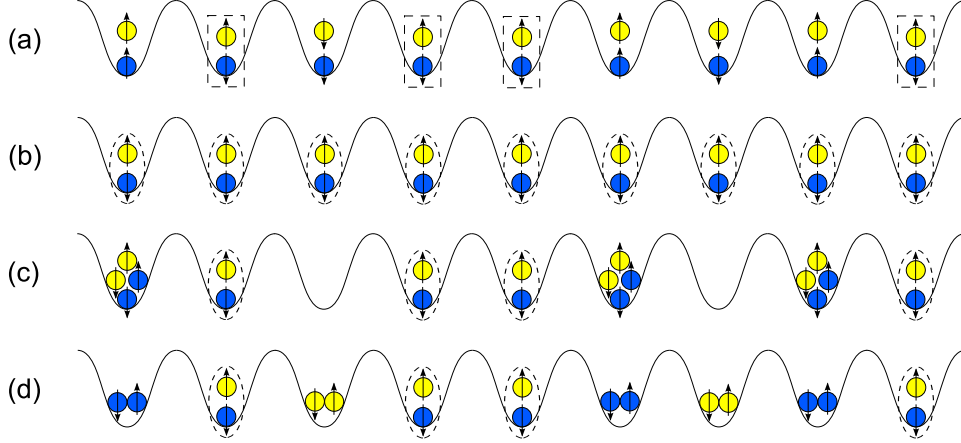


Fig. 4. (color online) The blue atoms are in the ground state, and the yellow color represents the excited state. (a): The RT phase displays alternating $S^z = \pm 1$ states with an arbitrary number of $S^z = 0$ (spin triplet) states in between; (b) the RS phase consists in spin singlets formed on each site by two atoms, one in the g state and the other in the e state. (c) the HC phase shows alternating $n_i = 4, 0$ states with an arbitrary number of singlets in between; (d) the HO phase exhibits alternating $(n_g - n_e)/2 = \pm 1$ states with again an arbitrary number of singlets in between.

2.2. Numerical approach

We now carry out numerical calculations using DMRG in order to investigate the various phase diagrams, and we focus on the half-filled case. For a finite system of size L , we can fix several quantum numbers: the total number of particles $Q_c = \sum_{i,l} n_{l,i} = 2L$, the z -component of the total spin of the whole system $S_{\text{tot}}^z = \sum_i (S_{e,i}^z + S_{g,i}^z)$, as well as the population difference between the two orbital levels $Q_o = \sum_i (n_{e,i} - n_{g,i})$. Typically, we keep up to 1600 states, which allow to have an error below 10^{-6} , and we use open boundary conditions (OBC).

The low-energy approach predicts seven insulating phases in the phase diagram. In order to identify the degenerate Mott phases (CDW, ODW, and SP), we compute local quantities (bond kinetic energy, local density, etc.). In order to detect non-degenerate Mott phases, we investigate the presence or absence of various edge states with quantum numbers $(Q_c, S_{\text{tot}}^z, Q_o)$, respectively equal to $(L, 1, 0)$, $(L+2, 0, 0)$, and $(L, 0, 1)$ for the RT, HC, and HO phases. The RS phase is identified as being non-degenerate and does not exhibit any kind of edge states with OBC.

The resulting zero-temperature phase diagrams are shown in Fig. 5 for two choices of V_{ex} . The overall topology of these two phase diagrams is in agreement with the low-energy results plotted in Fig. 2 since we confirm the presence of the seven insulating phases. There is a fair concordance for positive V_{ex} . However, there is a little discrepancy between the two approaches for negative V_{ex} : the small SP, HC and HO pockets do not match exactly. Still, we emphasize that the weak coupling phase diagram was obtained for much smaller values of $|V_{\text{ex}}|$; furthermore, the weak

coupling approach shows that the SP pocket shifts and then quickly disappears for increasing $|V_{\text{ex}}|$, in favor of the HC and HO phases. This indicates that the position of the SP pocket is not fully significant and strongly depends on the value of V_{ex} .

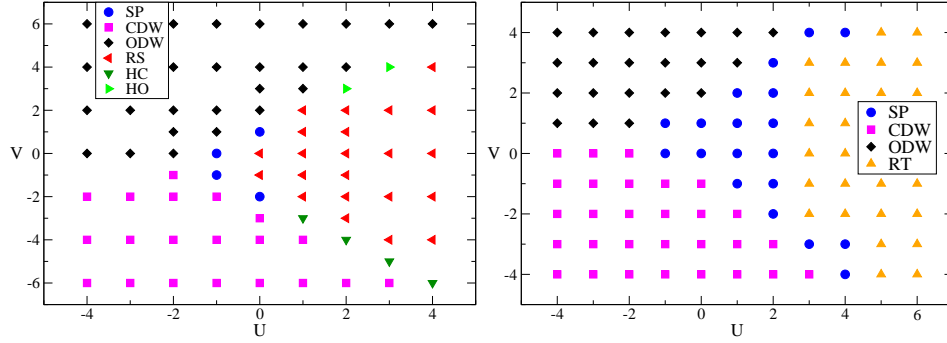


Fig. 5. Numerical phase diagram of model (1) at half-filling for $V_{\text{ex}} = -t$ (left) and $V_{\text{ex}} = t$ (right). We fix $t = 1$ as unit of energy.

3. Concluding remarks

We have investigated the phase diagram of ultracold 1D fermionic systems of earth-alkaline like atoms with nuclear spin ($I = 1/2$), at incommensurate filling and at half-filling. We showed that at incommensurate filling, while the charge degrees of freedoms remain gapless, the spin and orbital degrees of freedom are all gapped. The phase diagram displays four different phases with coexisting SP and CDW or with BCS instabilities.

At half-filling, seven Mott-insulating phases arise. Three of them are two-fold degenerate (SP, CDW, and ODW phases) and four are non-degenerate (RT, RS, HC, and HO phases). Among the non-degenerate phases, three are of the Haldane type (related to the physics of spin chains) and show hidden dilute order. We hope that, in the light of the recent experiments of earth-alkaline-atoms and ^{171}Yb atoms, future experiments will disclose part of the richness of the phase diagram presented in this paper.

References

1. B. J. DeSalvo, M. Yan, P. G. Mickelson, Y. N. Martinez de Escobar, and T. C. Killian, Phys. Rev. A **82**, 011608(R) (2010).
2. T. Fukuhara, Y. Takasu, M. Kumakura, and Y. Takahashi, Phys. Rev. Lett. **98**, 030401 (2007); S. Taie, Y. Takasu, S. Sugawa, R. Yamazaki, T. Tsujimoto, R. Murakami, and Y. Takahashi, *ibid* **105**, 190401 (2010).
3. A. V. Gorshkov, A. M. Rey, A. J. Daley, M. M. Boyd, J. Ye, P. Zoller, and M. D. Lukin, Phys. Rev. Lett. **102**, 110503 (2009).

4. A. V. Gorshkov, M. Hermele, V. Gurarie, C. Xu, P. S. Julienne, J. Ye, P. Zoller, E. Demler, M. D. Lukin, and A. M. Rey, *Nature Physics* **6**, 289 (2010).
5. M. A. Cazalilla, A. F. Ho, and M. Ueda, *New J. Phys.* **11**, 103033 (2009).
6. C. Xu, *Phys. Rev. B* **81**, 144431 (2010).
7. C. Wu, *Mod. Phys. Lett. B* **20**, 1707 (2006).
8. S. R. White, *Phys. Rev. Lett.* **69**, 2863 (1992); U. Schollwöck, *Rev. Mod. Phys.* **77**, 259 (2005).
9. A. O. Gogolin, A. A. Nersesyan, and A. M. Tsvelik, *Bosonization and Strongly Correlated Systems* (Cambridge University Press, Cambridge, England, 1998); T. Giamarchi, *Quantum Physics in One Dimension* (Clarendon press, Oxford, UK, 2004).
10. P. Azaria, A. O. Gogolin, P. Lecheminant, and A. A. Nersesyan, *Phys. Rev. Lett.* **83**, 624 (1999).
11. E. Boulat, P. Azaria, and P. Lecheminant, *Nucl. Phys. B* **822**, 367 (2009).
12. H. Nonne, E. Boulat, S. Capponi, and P. Lecheminant, *Phys. Rev. B* **82**, 155134 (2010).
13. H. Nonne, P. Lecheminant, S. Capponi, G. Roux, and E. Boulat, *Phys. Rev. B* **81**, 020408(R) (2010).